ISSN 1330–0016
CODEN FIZBE7

FIRST RESULTS FROM CLAS

LEE COLE SMITH

Physics Department, University of Virginia, Charlottesville, VA 22901, U.S.A.

Received 17 January 1999; Accepted 12 July 1999

The CEBAF Large Acceptance Spectrometer (CLAS) in Hall B has finished the first year of operation. CLAS subsystems, performance and preliminary results from the first production run are discussed.

PACS numbers: 07.77.+p, 13.60.-r UDC 539.126

Keywords: large acceptance spectrometer, photon reactions, electron reactions, energy 2 – 4 GeV

1. *Introduction*

The Continuous Beam Electron Accelerator Facility (CEBAF) at Jefferson Lab provides up to 6 GeV electrons to three experimental halls. Hall B houses the CEBAF Large Acceptance Spectrometer (CLAS), which is designed to study reactions induced by photons and electrons at luminosities up to 10^{34} cm^{-2}s^{-1}.

The physics program in Hall B has four major components:

- Electromagnetic excitation of baryon resonances
- Hyperon production
- Few-body properties of nuclei
- Polarized structure functions

All of these studies either need or can benefit from the capabilities offered by a large acceptance detector, namely: detection of multi-particle final states, limited luminosity, high coincidence background rejection and high relative accuracy.

Schematic views of the CLAS are shown in Figs. 1 and 2. Six superconducting coils generate a 2 Tesla toroidal magnetic field pointing primarily along ϕ. The space between the coils defines six wedge-shaped sectors which are individually instrumented as independent magnetic spectrometers. The detector package consists of drift chambers to determine the track of charged particles, gas Čerenkov counters for electron identification, plastic scintillation counters for measuring time-of-flight and sampling calorimeters to detect electromagnetic showers from electrons and photons.

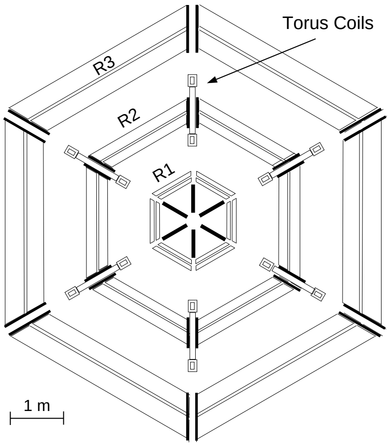

Fig. 1. Cross section view of CLAS, cut through the target. The cryostats housing the superconducting torus magnet divide the detector into six sectors. Coils of 'mini-torus' sweeping magnet are shown inside Region 1.

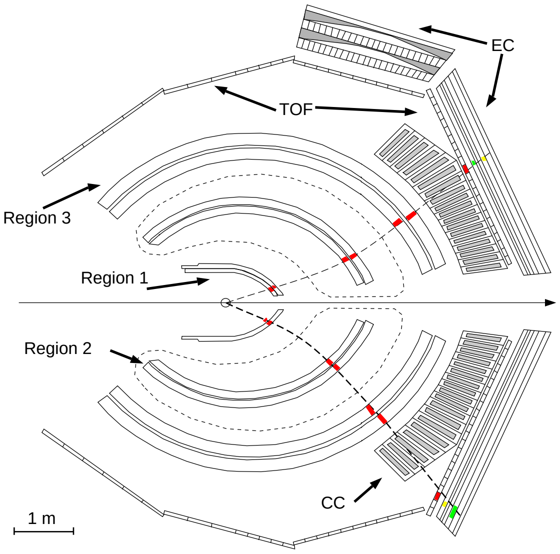

Fig. 2. Horizontal midplane cut through the CLAS detector at beam line elevation showing two charged particles traversing the drift chambers in opposite sectors. Outside of R3 are the remainder of the CLAS detectors including scintillators (TOF), calorimeters (EC) and Čerenkov counters (CC). The dotted lines show the projection of the torus coils on the midplane.

Within each sector, charged particles are tracked with 200 μm resolution by three arrays of multi-wire drift chambers. Region 1 is in the field-free volume surrounding the target, Region 2 in the central region of the field, and Region 3 just outside the coils. Axial wires parallel to the magnetic field together with stereo wires at a 6° angle sample each particle trajectory at up to 36 points. The sensitive region of the detector covers a polar angle range from 10° to 150°. Azimuthal coverage is approximately 80%, limited only by the magnet coils. For electron scattering experiments, a small normal-conducting toroid ('mini-torus') surrounding the target keeps low momentum charged electromagnetic background from reaching the Region 1 drift chamber.

Surrounding the drift chambers is an array of scintillation counters used to reconstruct the particle time-of-flight over the 5 meter flight path. This information is used together with the drift-chamber-derived momentum to calculate mass for particle identification. All counters have a phototube at both ends for improved timing and position resolution.

The threshold gas Čerenkov counters are sensitive to particles with $\beta \geq 0.998$. In combination with the electromagnetic calorimeters, electrons are detected with adequate suppression of π^-. The Čerenkov counters are located in front of the scintillation counters to minimize photon conversion and knock-on electrons.

The electromagnetic calorimeters provide electron identification over an energy range of 0.5 to 4.0 GeV, reconstruction of π^0, η, η', and Λ^* via detection of their 2γ decays, and neutron detection with high efficiency. Each module consists of alternating layers of lead sheets and plastic scintillator strips with both transverse and longitudinal sampling which allows energy measurements for electromagnetic particles with a resolution $\sigma_E/E \leq 0.1/\sqrt{E(\mathrm{GeV})}$. Angular resolution is ≤ 10 mrad. Six forward calorimeter modules provide coverage up to 45° in all 6 sectors; two additional modules cover the angular range up to 75°.

The hardware trigger is designed to accommodate all the above detector elements with many combinations of clustering and segmentation possible in order to isolate specific final states, reject background events and acquire calibration triggers in parallel with production triggers.

Beamline instrumentation includes a Faraday cup to determine the integrated electron flux, beam position monitors with 0.1 nA sensitivity, a Møller polarimeter to measure the polarization of the incident electron beam, and a bremsstrahlung tagging spectrometer for tagged-photon experiments. For photon running, the primary electron beam is deflected vertically into a low-power beam dump. A pair spectrometer and a total absorption counter located downstream of CLAS is then used to measure the photon beam flux.

2. *CLAS performance*

The performance criteria for CLAS provide a number of challenges both for accelerator operation and detector design. Operation of CLAS at the intended luminosity of 10^{34} requires the accelerator to provide stable beam currents to Hall

B at nanoamp levels while delivering up to 100 μA to the other experimental halls. From the detector point of view, the almost complete absence of passive shielding forced by the open geometry requires exceptionally clean beam profiles and careful tuning of sweeping magnet current and detector thresholds to minimize electromagnetic background triggers, maximize drift chamber lifetime and improve the overall quality of event reconstruction.

At the end of 1998, all performance criteria have been effectively met. Stable and reproducible beam tunes have been achieved with beam sizes less than 1 mm and beam halo contributions at the 10^{-3} level. Drift-chamber currents have been

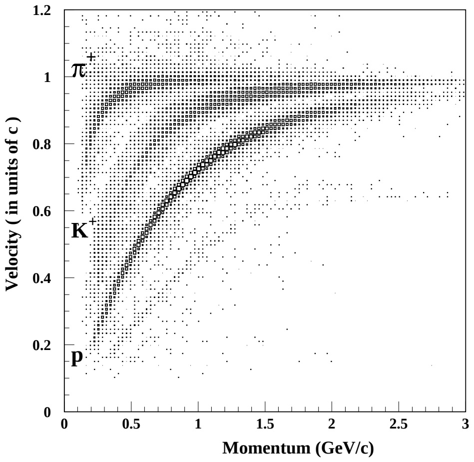

Fig. 3. Particle identification in CLAS. Momentum calculated from reconstructed drift chamber tracks is plotted against particle velocity, determined from TOF bars.

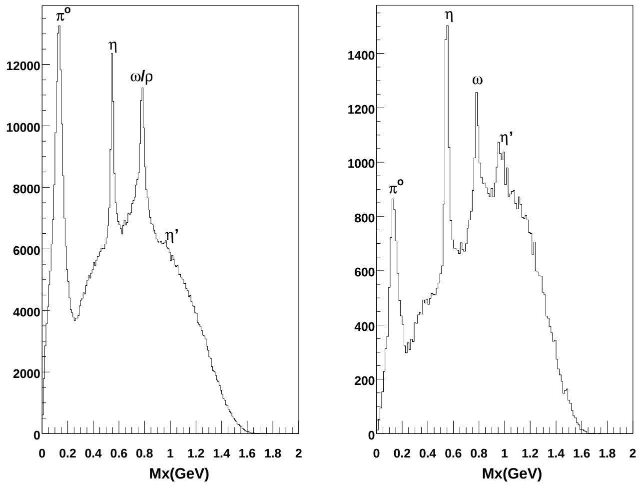

Fig. 4. Missing mass distributions for ep $\rightarrow$ e'pX*, where* X = *anything (left) and* X = *2 photons detected in electromagnetic calorimeter (right).*

reduced by more than two orders of magnitude at design luminosity by the active magnetic shielding provided by the mini-torus. Data acquisition speeds up to 2000 events/sec with almost deadtimeless operation is possible. Momentum resolution is better than 0.5% and time-of-flight resolution is better than 200 ps, which is adequate for separation of charged pions and kaons up to 2 GeV/c.

An example of charged particle identification is shown in Fig. 3. The momentum of positive particles emitted in coincidence with electrons in the process ep → e'X is plotted versus velocity measured in the time-of-flight (TOF) bars. The distribution shows clear contributions from pions, kaons, and protons; other bands from deuterons and tritons originate in the aluminum entrance and exit windows of the hydrogen cryo-target.

Missing mass is the primary method used to determine the 4-vectors of neutral particles in exclusive reactions, such as: ep → e'pπ^o, epη, eπ^+n or γp → K$^+\Lambda$, K$^+\Sigma^0$, K$^+\Lambda^*$. As an example, the left panel in Fig. 4 shows the missing-mass distribution for the process ep → e'pX. The missing-mass spectrum shows clear contributions from π^0, η, ρ, and ω production. Additionally requiring the detection of 2 photons in the calorimeters enhances the η' peak relative to the background, as the right panel shows.

Figure 5 shows the raw distributions of nucleon excitation energy W, for the

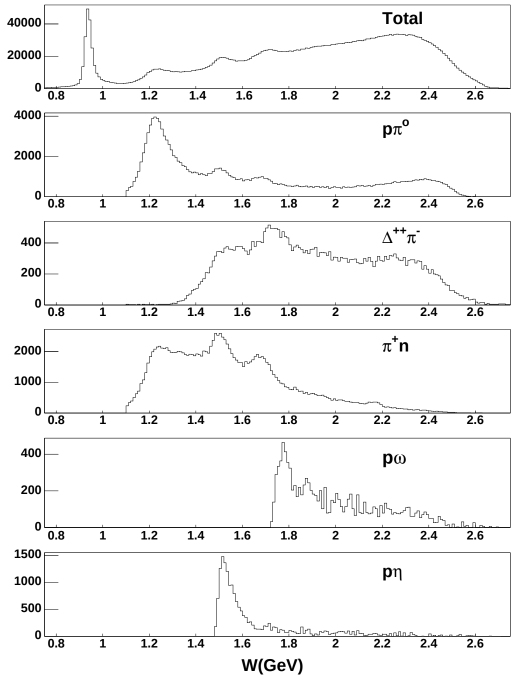

Fig. 5. Invariant mass distributions at 4 GeV *beam energy for reaction* ep → e'X, *where* X *is indicated for each panel. Top panel shows the total inclusive* W *distribution.*

total inclusive yield (top) and the yields for the pπ^o, $\Delta^{++}\pi^-$, π^+n, pω, and pη final states. These spectra have not been corrected for detector acceptance and efficiency. The data were taken during a single run, which provides a common normalization to all reaction channels and eliminates one of the main sources of systematic error.

3. *Preliminary results*

During 1998, 4 major production runs were executed for the following run groups:

- **e1** run (1.6, 2.4, and 4.0 GeV electrons on a hydrogen target, single arm trigger on inclusive electrons; physics motivation: mainly transition form factors for the nucleon resonances);
- **g1** run (tagged photons with $E_{\rm max} = 1.8$ and 2.5 GeV on a hydrogen target, triggered on a single charged particle in CLAS in coincidence with the tagging system; physics motivation: hyperon production, photocoupling of nucleon resonances);
- **g6** run (tagged photons with $E_{\rm max} = 4.0$ GeV on a hydrogen target, triggered on two charged particles in CLAS in coincidence with the tagging system; physics motivation: ϕ-photoproduction at large momentum transfer);
- **eg1** run (2.4 and 4.2 GeV polarized electrons on polarized protons and deuterons, single arm trigger on inclusive electrons; physics motivation: polarized asymmetries of nucleon resonances, GDH sum rule).

3.1. Elastic scattering

Data analysis from the first **e1** run period is far enough along that some preliminary results can be presented. One of the first checks on detector performance is elastic scattering on hydrogen, whose cross section in the Q^2 range of CLAS is already known at the 2% level from previous measurements at SLAC and elsewhere. A typical result is shown in Fig. 6, where the elastic yield from a 4.0 cm liquid hydrogen (LH$_2$) target over a range $0.85 < W < 1.05$ is plotted versus the electron scattering angle. The incident energy was $E_o = 1.645$ GeV and the corresponding Q^2 range is $0.35 < Q^2 < 1.0$. This good agreement with the radiatively-corrected cross section shows our normalization is under control at the 3-5% level. Further analysis is expected to refine this.

Unlike traditional electron spectrometers which require many angle settings, CLAS can accomodate measurements over a large angular range using a single setting of the magnetic field to select the Q^2 interval. Furthermore, the large momentum acceptance allows all electroproduction data taken with CLAS to include elastic scattering. Simultaneous measurements of elastic and inelastic scattering provide valuable checks for the calibration and performance of the detector including trigger efficiency, geometrical alignment and absolute cross sections. Events reconstructed outside physical kinematic regions can be used to estimate and monitor backgrounds, allowing a continuous check of the quality of the beam. Such results can also serve to cross-calibrate Monte-Carlo simulations of the detector response.

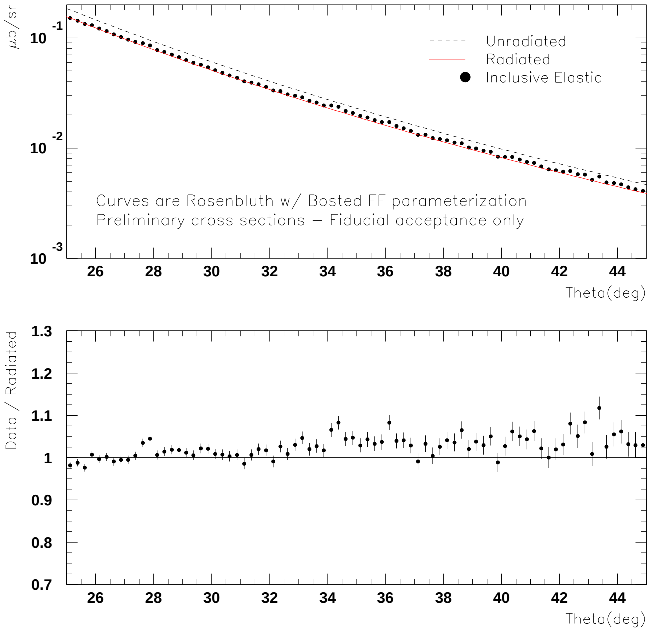

Fig. 6. Top: Elastic scattering cross section at $E_o = 1.645$ GeV *versus electron scattering angle. Comparison is made to Rosenbluth formula with and without radiative corrections. Electric and magnetic form factor parameterization of Bosted [1] is used. Bottom: Ratio of measured cross section to radiated Rosenbluth [2].*

3.2. Electroproduction of $\Delta(1232)$

Electroproduction of the $\Delta(1232)$ is a large component of a program to study the Q^2 evolution of the γNN* vertex for many of the low-lying nucleon resonances. For the Δ, this entails the simultaneous measurement of the ep $\rightarrow$ e'pπ^o and ep $\rightarrow$ e'nπ^+ reactions over the full azimuthal and polar angular ranges of the final state particles with high statistics. A partial wave decomposition of the decay products is then used to extract the resonant and nonresonant photon multipoles or helicity amplitudes. This information is expected to help resolve long-standing questions about the relevance of perturbative QCD to hadronic structure as well as to help isolate the correct framework in which to formulate models of non-perturbative QCD.

As an example, we present typical results from measurements of ep $\rightarrow$ e'pπ^o at 4.045 GeV. The top left panel of Fig. 7 show the raw counts from this reaction binned as a function of Q^2 and W. The CLAS acceptance is shown at top right.

The bottom-left panel shows the W dependence for various cuts in Q^2. Finally, the bottom-right panel shows the Q^2 falloff at the peak of the $\Delta(1232)$ compared to the dipole form factor.

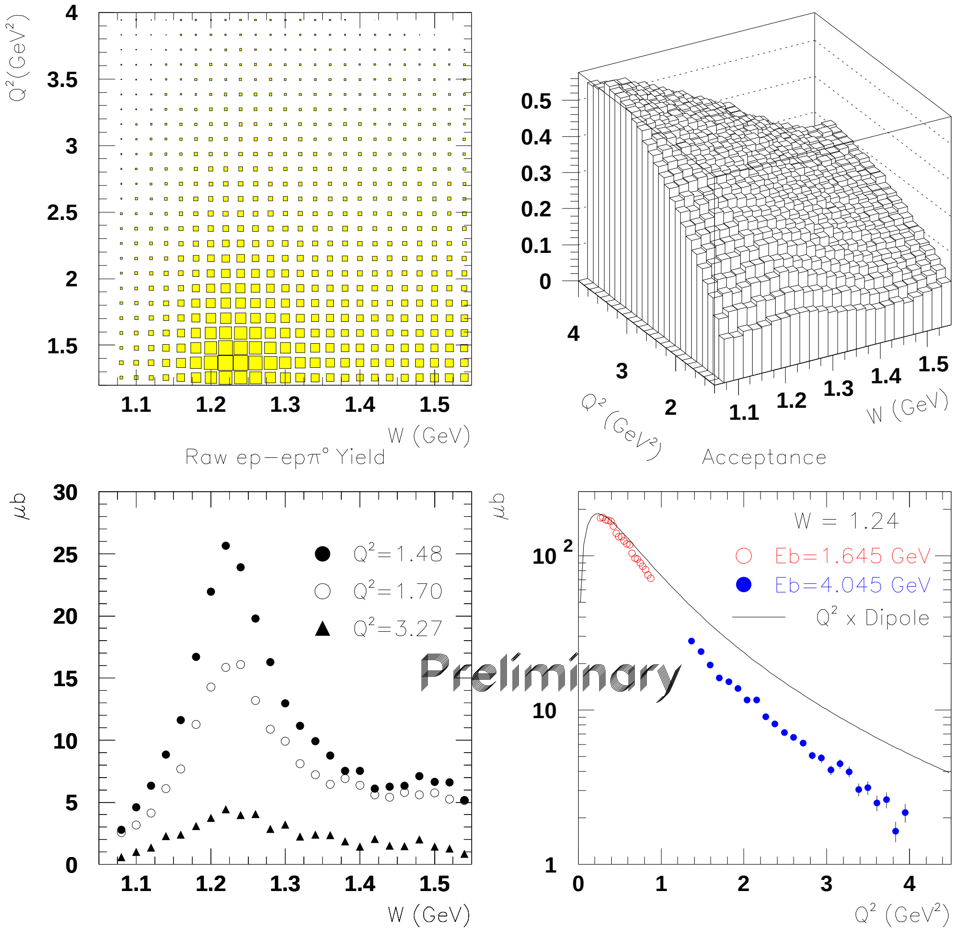

Fig. 7. Top left: Raw yield from ep → epπ^o *reaction at* E_o = 4.045 GeV. *Data are binned over* (Q^2,W) *range accepted by CLAS. Top right: CLAS acceptance for each* (Q^2,W) *bin. Bottom left: Invariant mass distribution for* Q^2 *bins shown. Bottom right:* Q^2 *distribution at peak of* $\Delta(1232)$ *resonance. Data from 1.645* GeV *beam energy also shown.*

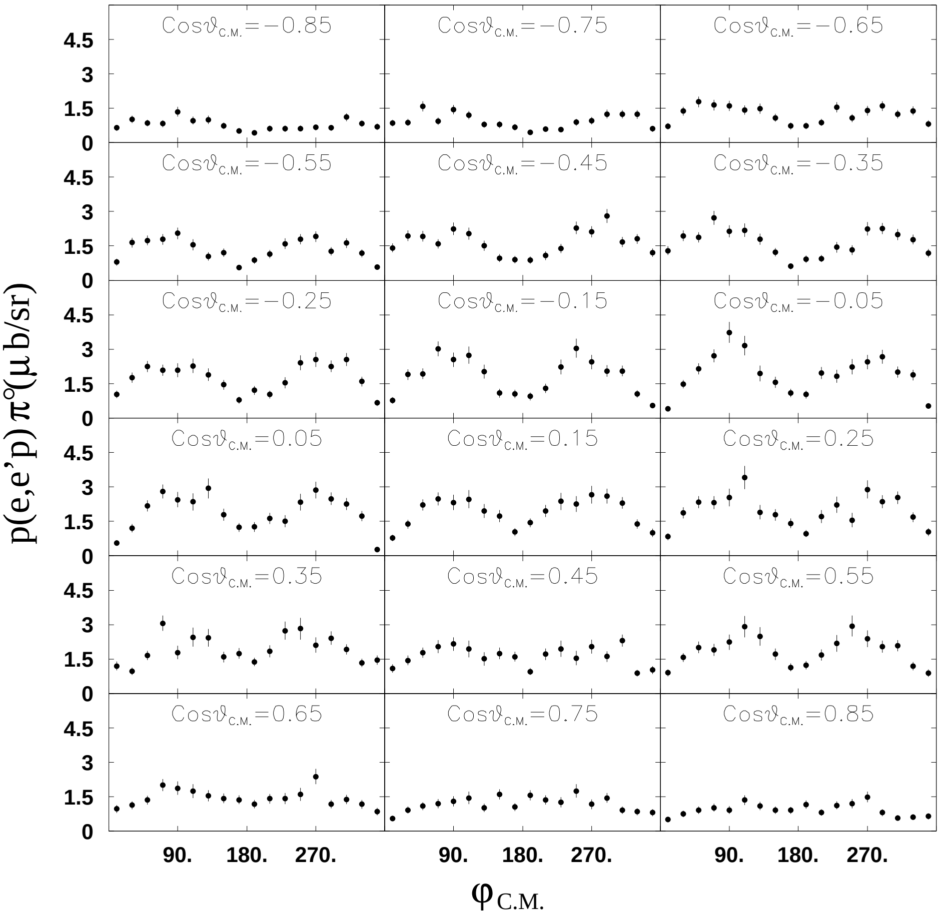

Fig. 8. Distribution of ϕ *in the* $\pi^o p$ *c.m. system for different bins of* $\cos\theta_{\rm cm}$*. Beam energy was 4.045* GeV*, and the data are binned over the interval* $1.2 < Q^2 < 1.9$ $\rm GeV^2$ *and* $1.25 < W < 1.3$ GeV*.*

With an unpolarized beam and target, the cross section depends on four structure functions and has the form

$$\sigma = \sigma_U + \epsilon\sigma_L + \epsilon\sigma_T \cos 2\phi + \sqrt{\frac{\epsilon(1+\epsilon)}{2}}\sigma_I \cos\phi \, ,$$

where ϵ is the longitudinal polarization factor for the virtual photon. The angle ϕ describes the rotation around the $\vec{q}$ direction of the $\pi-$N plane with respect to the electron scattering plane. By studying the dependence on ϵ and ϕ, the four structure functions can be separated. Figure 8 shows the ϕ dependence of the above cross section for various bins in $\theta_{\rm cm}$. The data clearly show the expected ϕ

dependence demanded by symmetry. The statistics represents about 10% of the run time approved for this particular program, although the sizes of the bins in Q^2, W will be smaller in the final analysis than presented here.

4. Summary

The CEBAF Large Acceptance Spectrometer, CLAS, has completed its first year of production running. Data have been taken with both electrons and photons and with polarized targets at beam energies up to 4.2 GeV. Exclusive channels have been measured over a Q^2 range of 0.1-4.0 GeV^2, and for nucleon excitations up to 2.5 GeV. Initial results indicate the detector is performing according to the design and that the data quality is good. Analysis projects are well underway and it is likely that results from CLAS will soon produce a wealth of new insights into the nature of quark confinement.

References

1) P. E. Bosted, Phys. Rev. C **51** (1995) 409;

2) M. N. Rosenbluth, Phys. Rev. **79** (1950) 615.

PRVI REZULTATI SUSTAVA CLAS

Spektrometar velikog kuta prihvaćanja u dvorani B u CEBAFu (CLAS) je u pogonu godinu dana. Raspravljaju se ispitivanja sustava, rad podsustava, i početni rezultati mjerenja.